Hydrol. Earth Syst. Sci. Discuss., 9, 3339–3384, 2012
www.hydrol-earth-syst-sci-discuss.net/9/3339/2012/
doi:10.5194/hessd-9-3339-2012

Hydrology and Earth System Sciences Discussions

Impact of climate change on sediment yield in the Mekong River Basin: a case study of the Nam Ou Basin, Lao PDR

B. Shrestha[1], M. S. Babel[1], S. Maskey[2], A. van Griensven[2,3], S. Uhlenbrook[2,4], A. Green[5], and I. Akkharath[5]

[1]Water Engineering and Management, School of Engineering and Technology, Asian Institute of Technology, P.O. Box 4, Klong Luang, Pathumthani 12120, Thailand
[2]Department of Water Science and Engineering, UNESCO-IHE Institute for Water Education, P.O. Box 3015, 261DA Delft, The Netherlands
[3]Department of Hydrology and Hydraulic Engineering, Vrije Universiteit Brussels, Pleinlaan 2, 1050 Brussels, Belgium
[4]Department of Water Resources, Delft University of Technology, P.O. Box 5048, 2600 GA Delft, The Netherlands
[5]Mekong River Commission Secretariat, Office of the Secretariat in Phnom Penh (OSP), P.O. Box 623, 576 National Road # 2, Sangkat Chak Angre Krom, Khan Menachey, Phnom Penh, Cambodia

Received: 21 February 2012 – Accepted: 3 March 2012 – Published: 14 March 2012

Correspondence to: B. Shrestha (bikeshs1983@gmail.com)

Published by Copernicus Publications on behalf of the European Geosciences Union.

HESSD

9, 3339–3384, 2012

Abstract

This paper evaluates the impact of climate change on sediment yield in the Nam Ou Basin located in Northern Laos. The Soil and Water Assessment Tool (SWAT) is used to assess future changes in sediment flux attributable to climate change. Future precipitation and temperature series are constructed through a delta change approach. As per the results, in general, temperature as well as precipitation show increasing trends in both scenarios, A2 and B2. However, monthly precipitation shows both increasing and decreasing trends. The simulation results exhibit that the wet and dry seasonal and annual stream discharges are likely to increase (by up to 15, 17 and 14 % under scenario A2; and 11, 5 and 10 % under scenario B2 respectively) in the future, which will lead to increased wet and dry seasonal and annual sediment yields (by up to 39, 28 and 36 % under scenario A2; and 23, 12 and 22 % under scenario B2 respectively). A higher discharge and more sediment flux are expected during the wet seasons, although the changes, percentage-wise, are observed to be higher during the dry months. In conclusion, the sediment yield from the Nam Ou Basin is likely to increase with climate change, which strongly suggests the need for basin-wide sediment management strategies in order to reduce the negative impact of this change.

1 Introduction

Climatic changes have been observed in the past decades and the changes have been predicted for the coming decades (IPCC, 2007). Climate models estimate that the global mean atmospheric temperature is likely to increase by 1.8 to 4.0° C by the end of the 21st century, depending on various greenhouse gas (GHG) emissions scenarios (IPCC, 2007). An increase in global temperature is expected to increase evapotranspiration and cause precipitation changes, which will significantly affect the hydrological regimes of many river systems (Lu, 2005). Many studies have shown that climate change could significantly affect streamflow (Nijssen et al., 2001; Menzel and

Burger, 2002), soil erosion rates (Pruski and Nearing, 2002; Michael et al., 2005; Neal et al., 2005) and sediment flux (Xu, 2003; Syvitski et al., 2005; Zhu et al., 2008). For instance, Zhu et al. (2008) have estimated the change in sediment flux from −0.7 to 13.7 % as a result of changes in rainfall from −0.7 to 17.8 % and temperature fluctuation of 0.03–2.4 °C in the Longchuanjiang catchment of the upper Yangtze River, China. Similarly, Pan et al. (2011) have reported 1 to 3 %, 3.9 to 11.4 % and −1.1 to −5.3 % changes in mean annual, wet season and dry season streamflows respectively and 1.2 to 4.7 %, 3.6 to 15.3 % and −1.3 to −7.7 % changes in mean annual, wet season and dry season sediment yields respectively for the Song Cau watershed in northern Vietnam due to the changes in precipitation and temperature under B1, B2, and A2 climate change scenarios.

The area under study for the effects of climate change in this research is one part of the Mekong River basin. The Mekong is the largest river in Southeast Asia and drains a catchment of 795 000 km^2 (Mekong River Commission, 2005) with China, Thailand, Laos, Cambodia, Vietnam and Myanmar as its riparian countries. Several climate change studies of the Mekong River basin have projected a likely increase in the basin's mean temperature and annual rainfall. For instance, Eastham et al. (2008) conducted a study to investigate the likely climate changes in the Mekong basin by the year 2030, and the results show a possible increase in the basin's mean temperature by 0.79 °C and a 13.5 % increase in annual precipitation resulting mainly from an increase in the wet season's (May to October) precipitation in all the sub-catchments. Apart from the climate change issue, the basin is currently facing other challenges too: the residential population is growing, urban sectors are expanding, and the economies of riparian countries are developing rapidly (Keskinen, 2008). Water-development projects, most notably the construction of large hydropower dams, are important for economic development (Mekong River Commission, 2006) and hence, extensive plans are underway to build reservoirs in the tributaries as well as the mainstream areas within the riparian countries (Mekong River Commission, 2008).

HESSD

9, 3339–3384, 2012

Impact of climate change on sediment yield in the Mekong River Basin

B. Shrestha et al.

The sediment load of a river is sensitive to both, climate change and a wide range of human activities within its drainage basin. These factors could influence sediment mobilization and transfer through actions like clearing of land, agricultural development, mineral extraction, urbanization and infrastructure development, dam and reservoir construction, and soil conservation and sediment control programs (Walling, 2008). Although the sediment of the Lower Mekong River has critical implications for aquatic ecology – fisheries, agriculture, water supply and river navigation, studies of the generation, transportation and deposition of sediment in the Lower Mekong are sparse (Wang et al., 2011). Previous studies (Ishidaira et al., 2008; Kiem et al., 2008; Hoanh et al., 2010; Kingston et al., 2011) of the hydrological impacts of potential climate changes in the Mekong have generally focused on discharge. The potential future changes in sediment load should be seen as an important requirement for sound river basin management (Walling, 2008). While researchers have highlighted the significant potential of climate change in increasing global soil erosion rates and possibly, consequent, increasing the amount of suspended sediment flux in rivers, the actual response of suspended sediment flux in a particular place varies because it is also highly affected by the physical characteristics of the catchment and human activities in it (SWCS, 2003; Zhang and Nearing, 2005). In any case, there is a clear need for improved understanding of the potential impact of climate change on the sediment load of the Mekong River specifically. Further, the possible changes in the sediment load needs to be evaluated in order to establish the sensitivity of the river system to the drivers of change, to understand the implications on future reservoir development and to assess their (the changes') effects on future management strategies (as outlined by Walling, 2008).

Reliable predictions of the quantity and rate of runoff, and sediment transport from land surfaces into streams, rivers and other water bodies are needed to help decision makers in developing watershed management plans for better soil and water conservation measures (Setegn et al., 2011) and to assess potential future implications due to the factors driving the changes. For this, several available mathematical models can be used. Of these, the Soil and Water Assessment Tool (SWAT) has been employed widely to evaluate the impact of climate change on soil erosion and sediment flux (Zhu et al., 2008). For example, Li et al. (2011) applied SWAT to evaluate the effect of temperature change on water discharge, and sediment and nutrient loading in the lower Pearl River basin, China. Hanratty and Stefan (1998) and Boorman (2003) have also described the application of SWAT to evaluate the impact of climate change on sediments in an agricultural watershed in Minnesota and in five European catchments.

The main objective of this paper is to evaluate the impact of possible climate change scenarios on the sediment yield in the Nam Ou River basin – one of the important sub-basins of the Mekong River basin. In this study, we have attempted to simulate the sediment yield from the Nam Ou basin and to quantify the implications of climate change on sediment load using the SWAT model. For assessing the impact of climate change, future temperature and precipitation time series were obtained by applying the change factor or delta change method (Hay et al., 2000) to a regional climate model (RCM) simulated temperature and precipitation.

2 Study area

The Nam Ou River basin, a sub-basin of the Mekong River basin, is located in the northern part of the Lao People's Democratic Republic (Fig. 1). It lies within 21°17′17″–22°30′40″ N and 101°45′47″–103°11′57″ E and covers a total area of 26 180.50 km^2. The topography of the basin is mostly mountainous, dominated by sharp relief. The elevation of the basin ranges from 263 to 2035 m a.m.s.l. (above mean sea level). The climate in the study area is characterized by two distinct seasons: a wet season (May to October) and a dry season (November to April). The mean annual temperature ranges from 20 to 26 °C. The basin receives about 1700 mm rainfall annually, of which about 80 % falls during the wet season. Woods and shrub land are the dominant land cover in the basin, and cover nearly 62 % of the total area. Soil in this river basin is predominantly sandy clay loam.

HESSD
9, 3339–3384, 2012

3 Data and methods

3.1 Observed data

Observed daily rainfall data from eleven stations (Luang Prabang, Xieng Ngeun, Muong Ngoy, Oudomxay, Muong Namtha, Phong Saly, Dien Bien, Lai Chau, Muong Te, Quynh Nhai, andTuan Giao), and climatic data of daily temperature, wind speed, humidity and solar radiation from three stations (Luang Prabang, Oudomxay and Phongsaly) were used for this study. The records for rainfall data were from 1980–2003, and for other climatic data the period was of 12 yr (1992–2003). The observed precipitation data at the stations were interpolated and aggregated to the sub-basin by using the MQUAD program in the Decision Support Framework of the Mekong River Commission (MRC). MQUAD generates estimations of areal rainfall (the catchment's average rainfall) by calculating a multi-quadratic surface from available point rain gauge data, such that the surface passes through all the gauge points. The surface is defined for a user specified area, consisting of one or more catchments, and is made up from a grid of estimated point rainfall values calculated by the software. The grid of point values calculated is then aggregated to produce a mean rainfall depth for each catchment. This process is repeated for each time step of the input point rainfall database.

The data of the maximum and minimum daily temperatures for 1980–1991 was derived from the 1/2-degree gridded global daily maximum and minimum temperature data, which is available for 1950 through 1999 from the Santa Clara University (SCU). Details of the SCU data can be found in Maurer et al. (2009). The source of this database is the following link: http://www.engr.scu.edu/~emaurer/global_data/. The statistics of the observed maximum and minimum monthly temperatures for three stations of the sub-basin were compared with the SCU data for the years 1992–1999, and this comparison is presented in Table 1. The comparison shows a good relationship between the observed and SCU data, with R^2 of 0.8 and above, and almost similar standard deviation. Table 1 also presents the linear relationship between the observed and SCU data. This relationship was used to derive the daily maximum and minimum temperature data for the 1980–1991 period.

The meteorological data, daily discharge (for 1992–2003) and suspended sediment concentration (SSC) data (for 1996–2002) from the gauging station at Muong Ngoy in the study area were obtained from the MRC Secretariat, Phonm Penh, Cambodia. Unlike discharge, which was measured daily, measurements of SSC were relatively sporadic, ranging from 6 to 56 measurements per year.

3.2 Regional climate model outputs

The RCM used in this study is PRECIS, developed by the Hadley Center of the UK Meteorological Office. The PRECIS RCM is based on the atmospheric components of the ECHAM4 GCM from the Max Planck Institute for Meteorology, Germany. The PRECIS data was produced by the Southeast Asian System for Analysis, Research and Training (START) Regional Center for 2225 grid cells covering the entire Mekong River basin with the resolution of $0.2 \times 0.2^{\circ}$ (approximately $22 \times 22\,\mathrm{km}^2$). This data, comprising two data sets for ECHAM4 SRES Scenarios A2 and B2, includes daily precipitation and maximum and minimum daily temperatures. The PRECIS RCM data over the periods of 1971–2000 (present) and 2011–2070 (future), for both A2 and B2 scenarios, was obtained from the Southeast Asian START Regional center. The source of this data base is the website http://www.start.or.th/. The specific boundary for the Nam Ou basin lies between latitudes 19.46°–22.77° N and longitudes 100.72°–103.32° E.

Many statistical downscaling techniques have been developed to translate large-scale GCM/RCM output into finer resolution (Fowler et al., 2007). In this study, the simplest method – change factor or delta change approach has been applied. The change factor or delta change method has been used in many climate change impact studies earlier (Hay et al., 2000; Diaz-Nieto and Wilby, 2005; Akhtar et al., 2008; Minville et al., 2008; Chen et al., 2011). Basically, this approach modifies the observed historical time series of precipitation by multiplying the ratio of the monthly future and actual precipitations simulated by a GCM or RCM for each time period. Similarly, the observed daily temperature is modified by adding the difference between the monthly future and actual temperatures as simulated by the GCM or RCM for each time period. The observational database used for this approach covers the period of 1981–2000 for both precipitation and temperature in this study.

3.3 The SWAT model description

SWAT is a river basin or watershed scale, semi-distributed, process-based, and continuous time hydrologic and water quality model initially developed by Arnold et al. (1993) and designed to evaluate the effect of land use management on water, sedimentation, and agricultural chemical yields in large complex watersheds which are heterogeneous in land use, soil and management conditions over a long period of time (Arnold et al., 1998; Neitsch et al., 2005). SWAT subdivides a watershed into different sub-basins connected by a stream network, and further into hydrological response units (HRUs). HRUs are the lumped land areas within the sub-basin that comprise of unique land cover, soil, slope and management combinations. SWAT simulates the hydrology of the watershed in two phases. The land phase of the hydrologic cycle controls the amount of water, sediment, nutrients and pesticides loadings to the main channel in each sub-basin. The water or routing phase of the hydrologic cycle controls the movement of water, sediment, nutrients and pesticide loadings through the channel network of the watershed into the outlet.

SWAT estimates the surface runoff volume from HRUs using the SCS curve number method (USDA-SCS, 1972) or the Green and Ampt infiltration method (Green and Ampt, 1911). In this study, the SCS curve number method has been used, which is a function of the soil's permeability, land use and antecedent soil water conditions as defined in SWAT. SCS defines three antecedent moisture conditions: dry (wilting point), average moisture, and wet (field capacity). SWAT calculates the peak runoff rate with a modified rational method. The model offers three options for estimating potential evapotranspiration: the Hargreaves (Hargreaves et al., 1985), Pristley-Taylor (Priestley

HESSD
9, 3339–3384, 2012

and Tyalor, 1972), and Penman-Monteith (Monteith, 1965) methods. The Penman-Monteith method has been used in this study. The model calculates the surface erosion within each HRU with the Modified Universal Soil Loss Equation (MUSCLE) (Williams, 1975). The MUSCLE is:

$$\text{sed} = 11.8 \times (Q_{\text{surf}} \times q_{\text{peak}} \times \text{area}_{\text{hru}})^{0.56} \times K_{\text{USLE}} \times C_{\text{USLE}} \times P_{\text{USLE}} \times LS_{\text{USLE}} \times \text{CFRG} \quad (1)$$

where sed is the sediment yield (metric tons day^{-1}), Q_{surf} is the surface runoff volume (mm ha^{-1} day^{-1}), q_{peak} is the peak runoff rate (m^3 s^{-1}), area$_{\text{hru}}$ is the area of the HRU (ha), K_{USLE} is the USLE soil erodibility factor, C_{USLE} is the USLE cover and management factor, P_{USLE} is the USLE support practice factor, LS_{USLE} is the USLE topographic factor and CFRG is the coarse fragment factor.

SWAT uses Manning's equation to define flow rate and velocity. Water is routed through the channel network using the variable storage routing method developed by Williams (1969) or the Muskingum routing methods which are variations of the kinematic wave model. For this study, the variable storage routing method was used. The sediment-routing model (Arnold et al., 1995) that simulates sediment transport in the channel network consists of two components operating simultaneously: deposition and degradation. The amount of deposition and degradation is based on the maximum concentration of sediment in the reach and the concentration of sediment in the reach at the beginning of the time step. The final amount of sediment in the reach is determined as:

$$\text{sed}_{\text{ch}} = \text{sed}_{\text{ch},i} - \text{sed}_{\text{dep}} + \text{sed}_{\text{deg}} \quad (2)$$

where sed$_{\text{ch}}$ is the amount of suspended sediment in the reach (metric tons day^{-1}), sed$_{\text{ch},i}$ is the amount of suspended sediment in the reach at the beginning of the time period (metric tons day^{-1}), sed$_{\text{dep}}$ is the amount of sediment deposited in the reach segment (metric tons day^{-1}), and sed$_{\text{deg}}$ is the amount of sediment reentrained in the reach segment (metric tons day^{-1}).

HESSD
9, 3339–3384, 2012

Impact of climate change on sediment yield in the Mekong River Basin

B. Shrestha et al.

The amount of sediment transported out of the reach is calculated as:

$$\text{sed}_{\text{out}} = \text{sed}_{\text{ch}} \times \frac{V_{\text{out}}}{V_{\text{ch}}} \tag{3}$$

where sed_{out} is the amount of sediment transported out of the reach (metric tons day^{-1}), sed_{ch} is the amount of suspended sediment in the reach (metric tons day^{-1}), V_{out} is the volume of outflow during the time step (m^3), and V_{ch} is the volume of water in the reach segment (m^3). The detailed descriptions of the different model components can be found in Neitsch et al. (2005).

The main input data for the SWAT model consists of daily precipitation, maximum and minimum air temperatures, wind speed, humidity, solar radiation, and spatial data on Digital Elevation Model (DEM), land use and soil. River discharge and suspended sediment yield were used for calibration and validation purposes. The input datasets for the model were obtained from the MRC Secretariat, Phonm Penh, Cambodia. In this study, a 250 m resolution DEM was used to delineate watershed and sub-basin boundaries, and to calculate sub-basin average slopes and to outline the stream network. Land use specifications, soil and slope layers were used to create HRUs within each sub-basin area.

3.3.1 Model calibration and validation

The Nam Ou SWAT model was calibrated and validated for streamflow but only calibrated for sediment yield. The periods 1992–1999 and 2000–2003 were used for streamflow calibration and validation respectively, including two years as a warm-up period. The warm-up period allows the model to cycle multiple times so as to minimize the effect of the user's estimates of initial state variables such as soil and water content and surface residue (Zhang et al., 2007). For this study, the sediment load was only calibrated for 1996–2002 due to the sporadic nature of data (only 176 measurements in 7 yr). For streamflow, the calibration was carried out both manually and automatically, while for sediment, only manual calibration was performed. For the automatic calibration of the SWAT model, the Sequential Uncertainty Fitting (SUFI-2) algorithm (Abbaspour et al., 2004, 2007) was used. SUFI-2 is a combined calibration and uncertainty analysis technique which expresses the total uncertainty of the model output in terms of final parameter ranges which also correspond to the model output ranges. Readers are referred to Abbaspour et al. (2007) for the details of SUFI-2 procedure.

3.3.2 Model evaluation and uncertainty analysis

The model performance is evaluated using the coefficient of determinant (R^2), the Nash-Sutcliffe (NS) measure (Nash and Sutcliffe, 1970) and Percent Bias (PBIAS). Several researchers (such as Santhi et al., 2001; Benaman et al., 2005) have suggested that the prediction efficiency of a calibrated model can be judged as satisfactory if NS and R^2 values are >0.6 (Setegn et al., 2010). PBIAS value <15 % is considered to be a satisfactory performance rating of a calibrated model by a number of researchers (Santhi et al., 2001; Van Liew et al., 2007).

The degree to which uncertainties are accounted for is quantified by a measure referred to as the *p*-factor, which is the percentage of measured data bracketed by the 95 % prediction uncertainty (95 PPU). The 95 PPU is calculated at 2.5 % and 97.5 % levels of the cumulative distribution of an output variable obtained through the Latin Hypercube Sampling method (Abbaspour et al., 2007), disallowing 5 % of the very bad simulations. Another measure quantifying the strength of a calibration/uncertainty analysis is the *r*-factor, which is the average thickness of the 95 PPU band divided by the standard deviation of the measured data. The goodness of fit and the degree to which the calibrated model accounts for the uncertainties are assessed by the closeness of the *p*-factor to 100 % (i.e. all observations falling inside the prediction uncertainty band) while having the narrowest band (*r*-factor → 0). The average distance between the upper and the lower 95 PPU is determined as:

$$\overline{d_x} = \frac{1}{k} \sum_{t=1}^{k} (X_\mathrm{U} - X_\mathrm{L})_l \quad (4)$$

HESSD
9, 3339–3384, 2012

$$r\text{-factor} = \frac{\overline{d_x}}{\sigma_x} \tag{5}$$

where X_U and X_L represent the upper and lower boundaries of the 95 PPU, and σ_x is the standard deviation of the measured data.

4 Results and discussion

4.1 Changes in temperature and precipitation

The present and future changes in simulated mean monthly, seasonal and annual maximum and minimum temperatures are presented in Tables 2a and b respectively. The results indicate a general increase in both, maximum and minimum temperatures, during the periods of 2011–2040 and 2041–2070 for scenarios A2 and B2. The change in mean monthly maximum and minimum temperature is predicted to be the highest in May, with a rise of 2.8 and 2.6 °C (respectively) under A2, while under B2, a higher maximum and minimum temperature shift is predicted for June (+2.1 °C) and September (+2.2 °C) respectively. At each horizon, the change in temperature is higher for the wet season as compared to the dry season, thereby indicating that warming will be stronger during the wet season. The mean annual maximum temperature rise ranges from 0.7 up to 1.9 °C over the period of 60 yr while the minimum temperature rise ranges from 0.8 up to 2.1 °C. The increase in average annual minimum temperature is predicted to be higher than the increase in maximum temperature in the basin.

Figure 2 and Tables 3a and b present a comparison of monthly mean rainfall for the present (1971–2000) and A2 and B2 scenarios. Under A2 scenario for the 2011–2040 horizon, precipitation rises for all months except January, while for 2041–2070, precipitation decreases from November to February and in May. The increase in precipitation is the highest for March (61.3 %) and the maximum decrease in precipitation will take place in January (56.2 %), as presented in Table 3a. Precipitation decreases for six months and increases for remaining months under scenario B2 for both horizons, with the highest increase taking place in March (47.7 %) and the highest decrease in January (51.3 %). The shift in peak rainfall from July to August is observed under A2 scenario, while for B2 scenario, this phenomenon is only obvious for the period of 2011–2040 (Fig. 2). The increase in precipitation can be seen in both seasons for both scenarios except for the dry season during the 2011–2040 horizon of B2 scenario where precipitation decreases by almost 6 %. For the 2011–2040 period, the change in precipitation during the dry season is greater than during the wet season. Mean annual precipitation over the basin is predicted to rise from 7.6 to 8.3 % under A2 scenario and from 3.6 to 5.7 % for B2 scenario. These results indicate that, in general, there will be an increase in the mean seasonal and annual precipitation over the basin.

Tables 3a and b also present future changes in maximum, 25th percentile, median and 75th percentile rainfall as compared to the present period (1971–2000) for both scenarios. The increase is observed for seasonal as well as annual rainfall. The increase in the maximum, 25th percentile, median and 75th percentile rainfall indicates that more intense rainfall events are to be expected in the future, which may result in increased high-flow events. Similarly, the increase in the 25th percentile, median and 75th percentile rainfalls during the dry season under A2 scenario implies that stream discharge may increase during the dry season.

4.2 Model calibration and validation

Table 4 presents the parameters that are used for the model calibration with their initial values/range and the calibrated values. The most sensitive parameters for flow predictions were found to be the base flow alpha factor (ALPHA_BF), recharge to deep aquifer (RCHRG_DP), curve number (CN2), channel effective hydraulic conductivity (CH_K2), available water capacity (SOL_AWC), Manning's "*n*" value for the main channel (CH_N2), surface runoff lag time (SURLAG), soil evaporation compensation factor (ESCO), saturated hydraulic conductivity (SOL_K), groundwater delay time (GW_DELAY) and canopy storage (CANMX). The most sensitive parameters for

HESSD
9, 3339–3384, 2012

sediment simulation were USLE land cover factor for wood and shrub land (WSEV), the linear re-entrainment parameter for channel sediment routing (SPCON), channel erodibility factor (Ch_COV1) and channel cover factor (Ch_COV2).

Figure 3a and b compare simulated daily streamflow with observed data for the calibration and validation periods respectively. The simulated daily flow matches the observed values for the calibration period with $R^2 = 0.64$, NS = 0.64 and PBIAS = 5.12 %. For the validation period, the simulated and observed daily flows showed acceptable agreement as indicated by the values of R^2, NS and PBIAS being 0.74, 0.72 and −14.25 % respectively. The results indicate that the Nam Ou SWAT model simulates the streamflow with reasonable accuracy. The model was able to replicate the base flow well for both, the calibration and validation, periods. However, the model was not able to capture peak flows except for 1998 and 1999 during the calibration period and for 2000 and 2003 during the validation period. This mismatch in peak flows might be attributed to precipitation data and also errors in the observed streamflow data, especially during high flows. The SWAT modeling study in the Mekong River basin carried out by Rossi et al. (2009) had also reported that errors in gauging stations can attribute to less reliable matching of hydrographs, especially at sites along the Mekong's tributaries. The errors in gauging stations vary across the flow range but are more pronounced at extreme low flows due to recording errors and at high flows due to rating errors (Rossi et al., 2009).

Figure 4 compares observed and simulated sediment yields. The R^2 and NS values are less than 0.6. However, the PBIAS value of 4.18 % indicates a good volume balance between simulated and observed sediment loads. The lower values of NS and R^2 may be attributed to limitations in terms of the continuity and length of the records. Potter and Hiatt (2009) also reported lower R^2 and NS values for the daily sediment calibration of the Laguna de Santa Rosa watershed in Northern California for similar reasons: a limited number of sediment samples for calibration. This lack also highlights the need for further investigation in the quality of the observed sediment data reflected from the sampling process and the method of sediment analysis. Any attempt to assess changes in the sediment load of a river system is largely dependent upon the number and the location of the measuring stations, the amount of available data, reliability, accuracy, the temporal resolution of the data and the length of the record (Walling, 2008).

Figure 4 also shows that the model was not able to capture peak sediment events. This under-prediction of peak events can be due to an uncertainty in the soil erosion model used in SWAT. SWAT simulates erosion based on the MUSLE, which was originally developed to estimate annual soil loss from agricultural fields. Also, the topographic factor (LS) derived from DEM may not be accurate due to inaccuracies in DEM (Babel et al., 2011). Jackson et al. (1986) and Johnson et al. (1986) reported that the MUSLE tends to over-predict sediment yields for small events and under-predict the same for large events. The studied watershed is located in a tropical climate zone with intense rainfall and heavy storms which have more potential to erode surface soil, but the MUSLE does not account for such factors (as is also mentioned by Phomcha et al.. 2011).

The *p*-factor, which is the percentage of observations bracketed by 95 PPU, brackets 72 % of the observations and *r*-factor equal to 0.49 for daily discharge, while for sediment yields, the *p*-factor and *r*-factor were 83 % and 0.68 respectively. Figures 5 and 6 show the uncertainty analysis results for monthly discharge and sediment yield of the study basin. As illustrated, a majority of the observed data is inside or very close to the predicted bands, thereby indicating good results. However, some peak events, mostly during the wet season (May–October), are outside the predicted bands for both discharge and sediment yields, and this implies the underestimation of these events by the model. For most cases, the uncertainty interval at the peaks is large. In general, the model performance, as represented by the *p*-factor and the *r*-factor, is reasonable. Large uncertainties in some events may also be due to possible errors in the observed data (as discussed above) or due to inadequate climate or landuse representations, as outlined by Schuol et al. (2008). This might also be due to the conceptual model uncertainties because each hydrological model suffers from conceptual model uncertainties and this is particularly true for large watershed models where many processes (natural or man-made) may not be adequately represented in the model (Schuol et al., 2008). In SUFI-2, the 95 PPUs are the combined outcome of the uncertainties in the conceptual model, parameters and input data. Nevertheless, these uncertainty sources are not separately evaluated but attributed as total model uncertainty to the parameters and are presented in the final parameter ranges and corresponding model output ranges. Overall, the results above indicate that the SWAT model can be applied for a reasonable assessment of the climate change impact on river discharge and sediment yield in the basin.

4.3 Impact of climate change on sediment yield

Figure 7a and b show the mean annual discharge cycle for the present and future climate for A2 and B2 scenarios and relative changes in mean future monthly discharges, as simulated by the SWAT model. The model simulation results show that for 2011–2040 under A2 scenario, the discharge increases in all months with the highest change for March and April (about 40 %) and lowest change taking place in January and February (less than 3 %). In contrast, for 2041–2070, the discharge is predicted to decrease during November–February and May–June with the maximum decrease in February and May (nearly 16 %). The highest change in discharge is observed for April, with a 35 % increase. There is an increase in river discharge during July–December and a decrease during January–June for 2011–2040 under B2 scenario. In April, the discharge is predicted to decrease by 25 %, which is the biggest change simulated by the model. For 2041–2070, there is an increase in the discharge in all the months except January and February. Interestingly, the highest change in discharge is observed in April, but in contrast to the 2011–2040 case, the discharge is predicted to increase by 26 %. The mean annual discharge cycle for the present and future climates for both scenarios shows the highest peak in August, predicted to increase by 16–26 % and 11–16 % for A2 and B2 scenarios respectively. Although the change is higher for April due to a larger percentage discharge change, more drastic changes in the magnitude

HESSD
9, 3339–3384, 2012

of streamflow are estimated for months in the wet season (mostly July–October). This suggests that the change will be more significant for the wet season than the dry season. The variability observed in the intra-annual (monthly) change of streamflow can be attributed to the variable changes in inter-annual rainfall. The changes in monthly temperature and precipitation show that an increase in temperature occurs for the basin in all the months of the year but changes in precipitation vary from month to month within the basin, and most probably from sub-basin to sub-basin.

In general, the model predicts an increase in the mean seasonal as well as the mean annual flow in the future for both scenarios (as presented in Table 5). Moreover, changes in the A2 scenario will be more than those in the B2 scenario. The mean wet and dry seasonal flows are predicted to increase by 1.09–1.15 and 1.03–1.17 times the present discharge rates respectively, leading to an overall increase (by 1.07–1.14 times the present discharge) in annual discharge. Therefore, the available water resources in the Nam Ou Basin can be expected to increase in the future. The increase in the wet season's flow indicates that there will be greater flood discharges. This further implies that in order to reduce the adverse effect of increased floods, proper flood water management strategies should be incorporated in the basin development plans. Also, the design and operation rules of the many reservoir dams that have been planned for hydropower purposes should be revisited in the light of these findings.

An increase in the dry season flow implies that more water will be available in the basin for that season's agricultural usage in Northern Laos. This is favorable to the 20-Yr Plan of the Lower Mekong Basin to increase the irrigation area during the dry season by 42.9 % in Northern Laos (Hoanh et al., 2010). Nevertheless, the increase in magnitude of discharge for the dry season is not so significant. Although changes in mean seasonal and annual discharge are important measures of change in a river system (as mentioned by Guo and Jiang, 2008), it is interesting to notice that, for the study area, the intra-annual (monthly) changes in the river's discharge are greater (from −26 to 42 % for A2 and −25 to 25 % for B2) as compared to the mean seasonal and annual discharge changes. The climate change impact study (using the

HESSD
9, 3339–3384, 2012

HadCM3 GCM) conducted by Kingston et al. (2011) in the Mekong River basin similarly observed greater changes in mean monthly river discharge (from −16 to 55 %). Such changes may be attributed to the complex and contrasting sub-basin changes in precipitation and evaporation, as outlined by Kingston et al. (2011). These results suggest that it is important for planners to keep in mind the monthly changes when devising any water management strategies for the future.

Figure 8a and b show the mean annual sediment yield cycle for the present and future climatic conditions for scenarios A2 and B2 and relative changes in the mean monthly sediment for the future. For the period of 2011–2040, the A2 scenario predicts a change in the mean monthly sediment yield that follows the same trend as the discharge with the largest percentage change for April (51 %). For the 2041–2070 period, the sediment yield decreases during March and increases during November–December, with the maximum change taking place in August (61 %); this being in contrast to the discharge change in same period. The change in intra-annual (monthly) sediment follows the same trend as discharge for the period of 2011–2040 for the B2 scenario. However, for the 2041–2070 period, the decrease in sediment yields by 26 % in March and the biggest change for September (almost 32 %) is observed in contrast to mean monthly discharge variations. Overall, the mean annual sediment cycle follows the trend of the mean annual discharge cycle. Streamflow increase in August by 16–26 % and 11–16 % for A2 and B2 scenario (respectively) is predicted to increase sediment yields by 34–61 % and 23–32 % (respectively). Further, it is interesting to notice that the intra-annual (monthly) changes in sediment yield range from −20 to 61 % for A2 and −53 to 35 % for B2, which are higher than the corresponding changes in discharge. This implies that the impact of climate changes on sediment yield is greater than on streamflow because sediment yield increases more than linearly with the flow (Naik and Jay, 2011).

Table 5 presents the climate change induced alterations in seasonal and annual sediment yields for the studied basin. As can be seen, both seasonal and annual sediment yields increase in the future, with higher changes in the A2 scenario. Under the A2 scenario, the increase in the wet season's sediment (24 to 39 %) and the dry season's sediment (12 to 28 %) will result in a 25 to 36 % rise in the annual sediment yield for the basin. Similarly, a 15 to 22 % rise in the annual sediment yield is predicted due to changes in sediment yields in the wet (17 to 23 %) and dry (−4 to 12 %) seasons under scenario B2. The medians, 25th percentiles, 75th percentiles and maximum values of annual sediment loads are also estimated to increase in the future, as shown in a box-whisker plot (Fig. 9). The results imply an overall increase in sediment loss from the basin in the future.

An increase in flow discharge will, in general, increase the mean monthly, seasonal and annual sediment loads, while a decrease in the flow discharge will decrease the sediment loads for all scenarios, which is similar to the findings of the climate change impact study conducted by Phan et al. (2011) in the Song Cau watershed in northern Vietnam. Most interestingly, for the 2041–2070 A2 scenario, in the months of November and December, sediment yield seems to increase even though water discharge decreases. For this period, the rainfall also decreases but temperature increases (+1.6° and +1.9 °C respectively). This suggests that the rise in temperature may increase soil loss. Through its influence on vegetation (Zhu et al., 2008; Li et al., 2011) and weathering (Zhu et al., 2011), increased temperature may aggravate the soil erosion rate, and consequently increase sediment flux. The study conducted by Li et al. (2011) in the lower Pearl River basin in China reported that an increase in temperature by 3 °C increases the sediment load by almost 14 %. For the 2041–2070 phase of the B2 scenario, during March, although discharge increases, the sediment decreases. For this month, both rainfall and temperature increase. This indicates that increased rainfall does not necessarily increase soil loss. For March, it is interesting to note that a 47 % increase in rainfall and nearly +2 °C shift in mean temperature results in less than 1 % increase in streamflow. This clearly proves the significant influence of increased evaporation in the hydrological process of a basin. The decrease in sediment flux may be due to the significant influence of increased evapotranspiration under warmer climate, as mentioned by Bogaart et al. (2003) in their study. Increased evapotranspiration may

HESSD
9, 3339–3384, 2012

offset and over-weigh increased rainfall and consequently reduce the erosion potential of rain. Nevertheless, the results indicate that the change of sediment yield and discharge in response to climate change do not always happen in the same direction. Changes in temperature and rainfall will affect the sediment transport capacity and erosion rate. This change in the sediment transport capacity and erosion rate causes changes in the sediment flux in a river, which is also outlined by Zhu et al. (2008).

Figure 10a shows the SWAT simulated sediment yield from various sub-basins of the study area for present climatic conditions. It is interesting to note that the northern and western sub-basins contribute most to sediment yield with an annual yield of more than 5 tons ha^{-1} yr^{-1}. Relative changes in annual average sediment yield from various sub-basins due to climate change are presented in Fig. 10b. Under scenario A2, the change varies from −10 to 80 %, with an increase of more than 20 % for most of the sub-basins. Interestingly, the lowermost sub-basins (18 and 19) show decreased sediment loss for both periods. Similarly, the change varies from −30 to 45 % for the B2 scenario. The southern sub-basins show decreased sediment yield. In conclusion, the change in precipitation and temperature is predicated to increase the sediment yield from most of the sub-basins, with the highest rise in northern sub-basins. Sediments are very important for the riverine ecosystems because of the attached nutrients. Increased sediments might change the nutrient loading into the river system, which can have significant implication on the water quality as well as the ecosystems.

Figure 11 is the longitudinal profile of the main stream, showing the locations of future reservoirs and their elevation relative to the basin outlet's datum. It also shows the averages of simulated annual sediment load (1971–2000) at future reservoir stations and changes in future sediment yield as compared to the 1971–2000 period under scenarios A2 and B2. Increase in mean annual sediment yield in each reservoir location has been observed. Increase in sediment yield is predicted to occur from less than 10 % to almost 60 %. In general, the change is higher in upstream dams and reduces as it moves downstream, which may be due to variations in the rate of change of rainfall and soil loss from subbasin to subbasin. Change in sediment yields due to climate

HESSD
9, 3339–3384, 2012

change in the future can have great implications for planned reservoirs and related sediment management. Increased sediment loads can intensify many problems linked to accelerated loss of reservoir storage through sedimentation and siltation or river channels and water distribution systems, an associated loss of conveyance capacity and increased turbidity of river water (Walling, 2008). Loss of reservoir storage can reduce the operational life and power generation capacity of the dam. This implies that there is a strong need for basin-wide sediment management strategies for the sustainability of the planned dams as well as for a robust river system.

5 Conclusions

This study assesses the impact of climate change on sediment yield in the Nam Ou basin located in the northern part of Laos. The regional climate model predictions show that, on a seasonal and annual scale, there is an overall increase in both temperature and precipitation in the future for both A2 and B2 scenarios. However, the changes in monthly precipitation show both, increasing and decreasing, trends.

A SWAT model was used to simulate the present and future changes in sediment yield in the study basin. Calibration, validation and uncertainty analyses for both, discharge and sediment, suggest that the SWAT model can be applied to simulate future changes in discharge and sediment yields due to eventual climate change. The delta change method or the change factor method was used as a downscaling method to generate future temperature and precipitation. Simulation results reveal that both seasonal and annual discharge will increase in the future, leading to an increased sediment yield. Variability was observed in the intra-annual (monthly) change of streamflow and sediment which can be attributed to the variable change in inter-annual rainfall. In general, higher discharge and sediment flux are expected during the wet season although the percentage changes were observed to be higher in the dry months. The climate's impact on sediment yield is larger than on streamflow and the changes do not always happen in the same direction. Overall results indicate that sediment loss from the basin will rise in the future.

The results of this study may be helpful to development planners, decision makers and other stakeholders when planning and implementing appropriate basin-wide sediment management strategies as well as water management strategies to adapt to climate change. Moreover, the statistics of future sediment flux will be quite significant for hydropower developers as they will enable planners to reassess the design, operation and sedimentation of future dams. Although the impact of sedimentation in future reservoirs in the Mekong and its downstream is an important issue, an accurate assessment of the same has been a big challenge due to the scarcity and scantiness of the observed data on sediment fluxes so far. Hence, the results of this study will also help planners devise more effective reservoir sediment management strategies.

The limitation of this study is that the uncertainties of RCM and erosion modeling have not been taken into account and landuse in the basin is assumed to remain the same in the future. Moreover, the change factor method used in this study does not modify the temporal and spatial structure of precipitation data (Diaz-Nieto and Wilby, 2005); hence, the changes in variance of future climate variables are not reflected in the paper.

Acknowledgements. The research presented in this paper is part of the PRoACC (Post-doctoral Programme on Climate Change Adaptation in the Mekong River basin) programme funded by the Netherlands Ministry of Development Cooperation (DGIS) through the UNESCO-IHE Partnership Research Fund. It was carried out jointly with UNESCO-IHE and Asian Institute of Technology, Thailand. It has not been subjected to peer and/or policy review by DGIS or UNESCO-IHE, and, therefore, does not necessarily reflect the views of these institutions. The authors would like to extend their appreciation to the Mekong River Commission for providing all the necessary data required for the study.

References

Abbaspour, K. C., Johnson, C. A., and Van Genuchten, M. T.: Estimating uncertain flow and transport parameters using a sequential uncertainty fitting procedure, Vadose Zone J., 3, 1340–1352, 2004.

Abbaspour, K. C., Yang, J., Maximov, I., Siber, R., Bogner, K., Mieleitner, J., Zobrist, J., and Srinivasan, R.: Modelling hydrology and water quality in the Pre-Alpine/Alpine Thur watershed using SWAT, J. Hydrol., 333, 413–430, 2007.

Akhtar, M., Ahmad, N., and Booij, M. J.: The impact of climate change on the water resources of Hindukush-Karakorum-Himalaya region under different glacier coverage scenarios, J. Hydrol., 355, 148–163, 2008.

Arnold, J. G., Allen, P. M., and Bernhardt, G.: A comprehensive surface-groundwater flow model, J. Hydrol., 142, 47–69, 1993.

Arnold, J. G., Williams, J. R., and Maidment, D. R.: Continuous-time water and sediment routing model for large basins, J. Hydraul. Eng., 121, 171–183, 1995.

Arnold, J. G., Srinivasan, R., Muttiah, R., and Willams, J. R.: Large area hydrological modeling and assessment part I: model development, J. Am. Water Resour. Assoc., 34, 73–89, 1998.

Babel, M. S., Shrestha, B., and Perret, S.: Hydrological impact of biofuel production: A case study of the Khlong Phlo Watershed in Thailand, Agr. Water Manage., 101, 8–26, 2011.

Benaman, J., Christine, A. S., and Douglas, A. H.: Calibration and validation of soil and water assessment tool on an agricultural watershed in upstate New York, J. Hydrol. Eng.-ASCE, 10, 363–374, 2005.

Bogaart, P. W., Van Balen, R. T., Kasse, C., and Vandenberghe, J.: Process-based modelling of fluvial system response to rapid climate change – I: model formulation and generic applications, Quaternary Sci. Rev., 22, 2077–2095, 2003.

Boorman, D. B.: Climate, Hydrochemistry and Economics of Surface-water Systems (CHESS): adding a European dimension to the catchment modeling experience developed under LOIS, Sci. Total Environ., 314–316, 411–437, 2003.

Chen, J., Brissette, F. P., and Leconte, R.: Uncertainty of downscaling method in quantifying the impact of climate change on hydrology, J. Hydrol., 401, 190–202, 2011.

Diaz-Nieto, J. and Wilby, R. L.: A comparison of statistical downscaling and climate change factor methods: impacts on low flows in the river Thames, United Kingdom, Climatic Change, 69, 245–268, 2005.

Eastham, J., Mpelasoka, F., Mainuddin, M., Ticehurst, C., Dyce, P., Hodgson, G., Ali, R., and Kirby, M.: Mekong River Basin Water Resources Assessment: Impacts of Climate Change, CSIRO: Water for a Healthy Country National Research Flagship, CSIRO, Australia, 2008.

Fowler, H. J., Blenkinsop, S., and Tebald, C.: Linking climate change modelling to impacts studies: recent advances in downscaling techniques for hydrological modeling, Int. J. Climatol., 27, 1547–1578, 2007.

Green, W. H. and Ampt, G. A.: Studies on soil physics, 1. The flow of air and water through soils, J. Agr. Sci., 4, 11–24, 1911.

Guo, H., Hu, Q., and Jiang, T.: Annual and seasonal streamflow responses to climate and land-cover changes in the Poyang Lake basin, China, J. Hydrol., 355, 106–122, 2008.

Hanratty, M. P. and Stefan, H. G.: Simulating climate change effects in a Minnesota agricultural watershed, J. Environ. Qual., 27, 1524–1532, 1998.

Hargreaves, G. L., Hargreaves, G. H., and Riley, J. P.: Agricultural benefits for Senegal River Basin, J. Irrig. Drain. Eng., 111, 113–124, 1985.

Hay, L. E., Wilby, R. L., and Leavesly, H. H.: Comparison of delta change and downscaled GCM scenarios for three mountainous basins in the United States, J. Am. Water Resour. Assoc., 36, 387–397, 2000.

Hoanh, C. T., Jirayoot, K., Lacombe, G., and Srinetr, V.: Impact of climate change and development on Mekong flow regime, First assessment-2009, MRC Technical Paper No. 29, Mekong River Comission, Vientiane, Lao PDR, 2010.

IPCC – Intergovernmental Panel on Climate Change: Climate change: AR4 synthesis report, Cambridge University Press, Cambridge, 2007.

Ishidaira, H., Ishikawa, Y., Funada, S., and Takeuchi, K.: Estimating the evolution of vegetation cover and its hydrological impact in the Mekong River basin in the 21st century, Hydrol. Process., 22, 1395–1405, 2008.

Jackson, W. L., Gebhardt, K., and Haveren, B. P. V.: Use of the modified universal soil loss equation for average annual sediment yield estimates on small rangeland drainage basin, in: Symposium on Drainage Basin Sediment Delivery, IASH, Albuquerque, New Mexico, USA, 1986.

Johnson, C. W., Gordon, N. D., and Hanson, C. L.: North-west rangeland sediment yield analysis by the MUSLE, T. Am. Soc. Agr. Biol. Eng., 26, 1889–1895, 1986.

Keskinen, M.: Water resources development and impact assessment in the Mekong Basin: which way to go?, Ambio, 37, 193–198, 2008.

HESSD

9, 3339–3384, 2012

Kiem, A. S., Ishidaira, H., Hapuarachchi, H. P., Zhou, M. C., Hirabayahi, Y., and Takeuchi, K.: Future hydroclimatology of the Mekong River basin simulated using the high-resolution Japan Meteorological Agency (JMA) AGCM, Hydrol. Process., 22, 1382–1394, 2008.

Kingston, D. G., Thompson, J. R., and Kite, G.: Uncertainty in climate change projections of discharge for the Mekong River Basin, Hydrol. Earth Syst. Sci., 15, 1459–1471, doi:10.5194/hess-15-1459-2011, 2011.

Li, Y., Chen, B.-M., Wang, Z.-G., and Peng, S.-L.: Effects of temperature change on water discharge, and sediment and nutrient loading in the lower Pearl River basin based on SWAT modeling, Hydrolog. Sci. J., 56, 68–83, 2011.

Lu, X. X.: Spatial variability and temporal change of water discharge and sediment flux in the lower Jinsha tributary: impact of environmental changes, River Res. Appl., 21, 229–243, 2005.

Maurer, E. P., Adam, J. C., and Wood, A. W.: Climate model based consensus on the hydrologic impacts of climate change to the Rio Lempa basin of Central America, Hydrol. Earth Syst. Sci., 13, 183–194, doi:10.5194/hess-13-183-2009, 2009.

Mekong River Commission: Overview of the Hydrology of the Mekong Basin, Mekong River Commission, Vientiane, 2005.

Mekong River Commission: Integrated Basin Flow Management, Social Team 2006 Final Report, Water utilization program – environment program, Mekong River Commission, Vientiane, 2006.

Mekong River Commission: Existing, Under Construction and Planned/Proposed Hydropower Projects in the Lower Mekong Basin, September 2008, Map produced by the Mekong River Commission (MRC), available online at: http://www.mrcmekong.org/programmes/hydropower.htm, last access: 10 September 2011, 2008.

Menzel, L. and Burger, G.: Climate change scenarios and runoff response in the Mulde catchment (Southern Elbe, Germany), J. Hydrol., 267, 53–64, 2002.

Michael, A., Schmidt, J., Enke, W., Deutschlander, T., and Maltiz, G.: Impact of expected increase in precipitation intensities on soil loss results of comapritive model simulations, Catena, 61, 155–164, 2005.

Minville, M., Brissette, F., and Leconte, R.: Uncertainty of the impact of climate change on the hydrology of a Nordic watershed, J. Hydrol., 358, 70–83, 2008.

Monteith, J. L.: Evaporation and the environment, in: The State and Movement of Water in Living Organisms, 19th Symposia of the Society for Experimental Biology, Cambridge University

HESSD

9, 3339–3384, 2012

Impact of climate change on sediment yield in the Mekong River Basin

B. Shrestha et al.

Press, London, UK, 205–234, 1965.
Naik, P. K. and Jay, D. A.: Distinguishing human and climate influences on the Columbia River: changes in mean flow and sediment transport, J. Hydrol., 404, 259–277, 2011.
Nash, J. E. and Sutcliffe, J. V.: River flow forecasting through conceptual models, Part I – a discussion of principles, J. Hydrol., 10, 282–290, 1970.
Neitsch, S. L., Arnold, J. G., Kiniry, J. R., and Williams, J. R.: Soil and Water Assessment Tool theoretical documentation, version 2005, Texas Water Resources Institute, College Station, Texas, USA, 2005.
Nijssen, B., O'Donnell, G., Hamlet, A., and Lettenmaier, D.: Hydrologic sensitivity of global rivers to climate change, Climate Change, 50, 143–175, 2001.
Phan, D. B., Wu, C. C., and Hsieh, S. C.: Impact of climate change on stream discharge and sediment yield in Northern Viet Nam, Water Resour., 38, 827–836, 2011.
Phomcha, P., Wirojanagud, P., Vangpaisal, T., and Thaveevouthti, T.: Predicting sediment discharge in an agricultural watershed: a case study of the Lam Sonthi watershed, Thailand, Sci. Asia, 37, 43–50, 2011.
Potter, C. and Haitt, S.: Modeling river flows and sediment dynamics for the Laguna de Santa Rosa watershed in Northern California, J. Soil Water Conserv., 64, 389–393, 2009.
Priestley, C. H. B. and Taylor, R. J.: On the assessment of surface heat flux and evaporation using large-scale parameters, Mon. Weather Rev., 100, 81–92, 1972.
Pruski, F. E. and Nearing, M. A.: Climate-induced changes in erosion during the 21st century for eight U.S. locations, Water Resour. Res., 38, 34-1–34-11, 2002.
Rossi, C. G., Srinivasan, R., Jirayoot, K., Duc, T. L., Souvannabouth, P., Binh, N., and Gassman, P. W.: Hydrologic evaluation of the Lower Mekong River basin with the soil and water assessment tool model, Int. Agr. Eng. J., 18, 1–13, 2009.
Santhi, C., Arnold, J. G., Williams, J. R., Dugas, W. A., Srinivasan, R., and Hauck, L. M.: Validation of the SWAT model on a large river basin with point and nonpoint sources, J. Am. Water Resour. Assoc., 37, 1169–1188, 2001.
Schuol, J., Abbaspour, K. C., Srinivasan, R., and Yang, H.: Estimation of freshwater availability in the West African sub-continent using the SWAT hydrologic model, J. Hydrol., 352, 30–49, 2008.
Setegn, S.G., Dargahi, B., Srivivasan, R., and Melesse, A. M.: Modeling of sediment yield from Anjeni-Gauged watershed, Ethiopia using SWAT model, J. Am. Water Resour. Assoc., 46, 514–526, 2010.

HESSD
9, 3339–3384, 2012

SWCS: Conservation implications of climate change: soil erosion and runoff from cropland, Soil and Water Conservation Society, Ankeny, 2003.
Syvitski, J. P. M., Kettner, A. J., Peckham, S. D., and Kao, S. J.: Predicting the flux of sediment to the coastal zone: application to the Lanyang watershed, Northern Taiwanm, J. Coast. Res., 21, 580–587, 2005.
USDA-SCS – United States Department of Agriculture – Soil Conservation Service: National engineering handbook, Section 4 Hydrology, Chapter 4–10, USDA-SCS, Washington, USA, 1972.
Van Liew, M. W., Veith, T. L., Bosch, D. D., and Arnold, J. G.: Suitability of SWAT for the conservation effects assessment project: A comparison on the USDA-ARS experimental watersheds, J. Hydrol. Eng.-ASCE, 12, 173–189, 2007.
Walling, D. E.: The changing sediment load of the Mekong River, Ambio, 37, 150–157, 2008.
Wang, J. J., Lu, X. X., and Kummu, M.: Sediment load estimates and variations in the Lower Mekong River, River Res. Appl., 27, 33–46, 2011.
Williams, J. R.: Flood routing with variable travel time or variable storage coefficients, T. ASAE, 12, 100–103, 1969.
Williams, J. R.: Sediment-yield prediction with universal equation using runoff energy factor, Present and Prospective Technology for Predicting Sediment Yield and Sources: Proceedings of the Sediment Yield Workshop, ARS-S-40, 28–30 November 1972, USDA Sedimentation Lab., Oxford, Mississippi, 244–252, 1975.
Xu, J. X.: Sediment flux to the sea as influenced by changing human activities and precipitation: example of the Yellow River, China, Environ. Manage., 31, 328–341, 2003.
Zhang, X., Srinivasan, R., and Hao, F.: Predicting hydrologic response to climate change on the Luohe River Basin using the SWAT model, Am. Soc. Agr. Biol. Eng., 50, 901–910, 2007.
Zhang, X. C. and Nearing, M. A.: Impact of climate change on soil erosion, runoff, and wheat productivity in central Oklahoma, Catena, 61, 185–195, 2005.
Zhu, Y.-M., Lu, X. X., and Zhou, Y.: Sediment flux sensitivity to climate change: a case study in the Longchuanjiang catchment of the upper Yangtze River, China, Global Planet. Change, 60, 429–442, 2008.

HESSD
9, 3339–3384, 2012

Table 1. Comparison and relationship between observed and Santa Clara University (SCU) simulated monthly temperature data for the 1992–1999 period.

Stations	R^2	Standard error	Mean (°C)		Standard deviation (°C)		Relationship between monthly observed and Santa Clara simulated data
			Observed	Santa Clara	Observed	Santa Clara	
				T_{max}			
Luang Prabang	0.8	1.3	31.3	27.6	3.0	2.3	Obs. tmax = 1.1596 SCU tmax – 0.6673
Oudomxay	0.9	0.9	28.8	27.3	2.6	2.5	Obs. tmax = 0.9657 SCU tmax + 2.4270
Phong Saly	0.8	1.3	23.7	26.1	3.0	2.9	Obs. tmax = 0.9597 SCU tmax – 1.4027
				T_{min}			
Luang Prabang	0.8	1.7	20.0	17.2	3.9	3.7	Obs. tmin = 0.9679 SCU tmin + 3.3511
Oudomxay	0.9	1.1	17.0	17.0	4.7	3.9	Obs. tmin = 1.1793 SCU tmin – 3.0752
Phong Saly	0.8	1.3	16.2	16.2	2.9	4.1	Obs. tmin = 0.6526 SCU tmin + 5.549

HESSD
9, 3339–3384, 2012

Table 2a. Changes in mean monthly wet (May –October) and dry (November–April) seasonal and annual maximum temperatures under scenarios A2 and B2 relative to 1971–2000 (units in °C).

Period	Scenario	Month												Season		Annual
		Jan	Feb	Mar	Apr	May	Jun	Jul	Aug	Sep	Oct	Nov	Dec	Wet	Dry	
1971–2000	Present	21.8	24.4	27.0	28.4	28.0	27.6	27.3	27.3	27.5	25.7	23.5	20.8	27.2	24.3	25.8
Shift compared to base case																
2011–2040	A2	0.6	0.4	−0.5	0.4	0.7	1.0	1.2	1.0	1.2	1.2	0.7	0.6	1.1	0.4	0.7
2011–2040	B2	0.3	0.1	0.0	1.2	0.8	1.6	1.0	0.9	0.9	1.5	0.7	0.4	1.1	0.5	0.8
2041–2070	A2	1.9	1.4	1.5	1.5	2.8	2.3	1.9	1.5	1.8	2.5	1.7	1.8	2.1	1.6	1.9
2041–2070	B2	1.6	1.4	1.4	1.3	1.2	2.1	1.5	1.4	1.8	2.0	1.3	1.4	1.7	1.4	1.5

Table 2b. Changes in mean monthly wet (May–October) and dry (November–April) seasonal and annual minimum temperatures under scenarios A2 and B2 relative to 1971–2000 (units in °C).

Period	Scenario	Month												Season		Annual
		Jan	Feb	Mar	Apr	May	Jun	Jul	Aug	Sep	Oct	Nov	Dec	Wet	Dry	
1971–2000	Present	11.2	11.9	14.2	16.9	19.0	20.5	20.5	20.1	19.3	17.6	14.9	11.5	19.5	13.4	16.5
Shift compared to base case																
2011–2040	A2	0.5	0.7	0.5	0.8	0.9	1.0	1.0	1.0	1.1	1.2	0.6	0.5	1.0	0.6	0.8
2011–2040	B2	0.5	0.6	0.6	1.2	1.1	1.3	1.1	1.0	1.2	1.1	0.8	0.2	1.1	0.7	0.9
2041–2070	A2	1.6	1.5	2.3	2.3	2.6	2.1	2.1	2.1	2.3	2.2	1.4	2.0	2.2	1.9	2.1
2041–2070	B2	1.3	1.4	2.1	2.1	1.7	1.9	1.7	1.8	2.2	1.6	1.4	1.3	1.8	1.6	1.7

HESSD
9, 3339–3384, 2012

Impact of climate change on sediment yield in the Mekong River Basin

B. Shrestha et al.

Table 3a. Changes in mean monthly wet (May–October) and dry (November–April) seasonal and annual precipitation statics (mean, maximum, 25th percentile, median and 75th percentile) under scenario A2 relative to 1971–2000.

Period	Statics	Month												Season		Annual
		Jan	Feb	Mar	Apr	May	Jun	Jul	Aug	Sep	Oct	Nov	Dec	Wet	Dry	
1971–2000	Mean (mm)	23	30	63	149	222	262	329	322	170	96	53	15	1401	333	1735
	Max (mm)	101	101	275	443	398	421	499	503	397	241	153	87	1824	676	2320
	25th percentile (mm)	33	44	83	184	262	329	364	397	176	100	81	25	1545	422	1949
	Median (mm)	19	19	53	145	220	254	324	317	165	77	39	8	1347	326	1699
	75th percentile (mm)	3	12	27	72	174	219	290	237	141	56	17	3	1254	227	1588
							Change (%)									
2011–2040	Mean	−24.7	10.8	61.3	27.2	4.3	0.6	1.1	11.2	6.2	5.0	1.4	8.2	4.7	23.7	8.3
	Max	−50.9	35.5	−11.6	−0.7	4.2	−3.2	5.4	11.1	−0.6	5.1	−3.0	17.8	4.4	−6.4	2.3
	25th percentile	−23.1	7.6	55.1	32.5	8.8	−0.1	−1.6	11.7	4.4	9.0	−1.8	8.1	5.5	16.3	10.4
	Median	5.7	0.4	48.4	27.1	1.1	3.6	0.9	7.7	2.0	4.0	5.3	15.3	5.3	36.5	8.5
	75th percentile	−28.2	−2.8	104.2	50.2	8.0	0.5	−2.5	9.2	6.2	4.8	8.9	21.5	5.0	42.8	8.1
2041–2070	Mean	−56.2	−7.4	48.2	17.8	−18.9	0.0	15.8	22.0	14.6	5.4	−36.1	−9.1	7.9	6.4	7.6
	Max	−69.8	−16.0	−16.1	0.7	−13.1	4.6	21.2	36.7	19.4	25.4	−23.8	−2.3	17.2	−15.8	11.7
	25th percentile	−51.8	−4.0	50.2	38.2	−16.7	3.1	17.9	15.0	18.5	4.5	−41.8	−27.9	6.5	4.7	5.7
	Median	−62.1	−12.1	44.1	−6.7	−18.2	−0.1	18.7	10.6	13.8	15.5	−35.2	−22.3	10.6	14.3	10.4
	75th percentile	−51.7	−32.3	108.0	56.1	−13.4	1.6	8.6	29.3	17.0	24.9	−12.6	−24.2	8.3	10.6	4.1

HESSD
9, 3339–3384, 2012

HESSD

9, 3339–3384, 2012

Impact of climate change on sediment yield in the Mekong River Basin

B. Shrestha et al.

Table 3b. Changes in mean monthly wet (May–October) and dry (November–April) seasonal and annual precipitation statics (mean, maximum, 25th percentile, median and 75th percentile) under scenario B2 relative to 1971–2000.

Period	Statics	Month												Season		Annual
		Jan	Feb	Mar	Apr	May	Jun	Jul	Aug	Sep	Oct	Nov	Dec	Wet	Dry	
1971–2000	Mean (mm)	23	30	63	149	222	262	329	322	170	96	53	15	1401	333	1735
	Max (mm)	101	101	275	443	398	421	499	503	397	241	153	87	1824	676	2320
	25th percentile (mm)	33	44	83	184	262	329	364	397	176	100	81	25	1545	422	1949
	Median (mm)	19	19	53	145	220	254	324	317	165	77	39	8	1347	326	1699
	75th percentile (mm)	3	12	27	72	174	219	290	237	141	56	17	3	1254	227	1588
							Change (%)									
2011–2040	Mean	−51.0	−1.1	13.2	−9.0	4.8	−4.4	7.2	11.6	9.8	4.8	−2.1	−9.5	5.8	−5.9	3.6
	Max	−69.8	7.3	−17.6	−24.1	7.0	−4.7	4.6	15.0	3.1	7.6	15.8	11.6	6.9	−19.0	1.9
	25th percentile	−50.5	3.7	17.0	−9.6	5.0	−6.3	4.7	11.6	7.7	12.3	0.0	−26.9	7.5	−3.5	3.3
	Median	−32.3	2.4	19.1	−7.9	2.4	−1.2	8.8	8.9	5.3	2.9	−10.6	−27.3	6.2	−0.1	4.6
	75th percentile	−52.5	−23.6	30.1	0.8	3.1	−4.6	7.9	8.8	9.9	4.7	−13.6	−19.9	5.6	6.5	2.7
2041–2070	Mean	−51.3	−26.6	47.7	11.4	8.0	−2.5	8.1	7.1	12.9	−2.9	−3.7	−45.4	5.7	5.6	5.7
	Max	−60.0	−18.2	−13.7	1.9	17.8	5.7	10.1	12.1	15.6	11.0	23.6	−58.6	14.5	−3.2	11.9
	25th percentile	−40.5	−21.3	47.0	29.3	12.3	−0.5	7.8	8.4	14.4	−6.0	−13.5	−49.8	3.7	9.3	3.3
	Median	−66.8	−27.1	41.2	−6.3	5.2	−0.9	12.3	2.9	12.1	7.6	−9.0	−36.4	7.4	5.8	7.4
	75th percentile	−47.4	−47.0	107.5	28.9	11.5	−4.0	6.6	10.5	16.0	11.5	26.4	−43.1	6.9	−7.9	0.3

Table 4. Calibrated values of adjusted parameters.

Variable	Parameter name	Description and units	Initial value/ range	Fitted parameter value
Flow	ALPHA_BF	Baseflow alpha factor	0.048	0.81
	RCHRG_DP	Deep aquifer percolation fraction	0.05	0.085
	CN2	Curve number	48.91–80	+1.89 %
	CH_K2	Channel effective hydraulic conductivity (mm h^{-1})	0	3.15
	SOL_AWC	Available water capacity (mm mm^{-1} soil)	0.10–0.28	+26.10 %
	CH_N2.	Mannings's "*n*" value for main channel	0.014	0.19
	SURLAG	Surface runoff lag (days)	4	11.69
	ESCO	Soil evaporation compensation factor	0.95	0.83
	SOL_K	Saturated hydraulic conductivity (mm h^{-1})	2.07–6.50	60.69 %
	GW_DELAY	Groundwater delay time (days)	31	51.79
	CANMX	Canopy storage (mm)	0	2.04
Sediment	Usle_C (WSEV*)	USLE land cover factor	0.001	0.05
	SPCON	Linear re-entrainment parameter for channel sediment routing	0.0001	0.0025
	Ch_COV1	Channel erodibility factor	0	0.50
	Ch_COV2	Channel cover factor	0	0.18

*WSEV means Wood Shurb Evergreen Vegetation.

Discussion Paper | Discussion Paper | Discussion Paper | Discussion Paper |

HESSD

9, 3339–3384, 2012

Impact of climate change on sediment yield in the Mekong River Basin

B. Shrestha et al.

Table 5. Changes in wet (May–October) and dry (November–April) seasonal, and mean annual discharge and sediment yield under Scenarios A2 and B2, relative to 1971–2000.

	Mean discharge ($m^3 s^{-1}$) 1971–2000	Change in discharge (fraction)				Mean sediment yield (tons) 1971-2000	Change in sediment yield (fraction)			
		2011–2040		2041–2070			2011–2040		2041–2070	
		A2	B2	A2	B2		A2	B2	A2	B2
Wet	1041	1.13	1.09	1.15	1.11	1 058 147	1.24	1.17	1.39	1.23
Dry	174	1.17	0.99	1.03	1.05	114 576	1.28	0.96	1.12	1.12
Annual	607	1.13	1.07	1.14	1.10	586 362	1.25	1.15	1.36	1.22

HESSD
9, 3339–3384, 2012

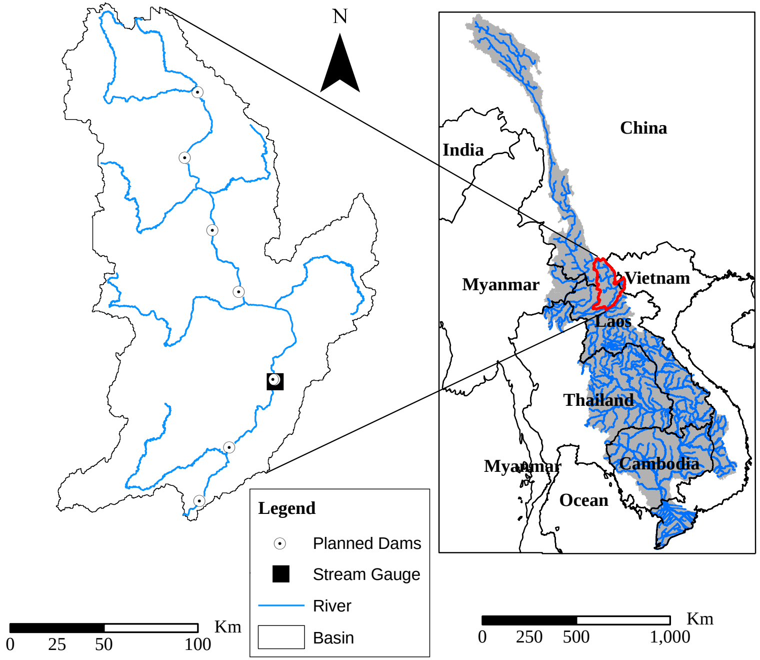

Fig. 1. Location map of the study area, stream gauge and location of planned dams.

HESSD
9, 3339–3384, 2012

Impact of climate change on sediment yield in the Mekong River Basin

B. Shrestha et al.

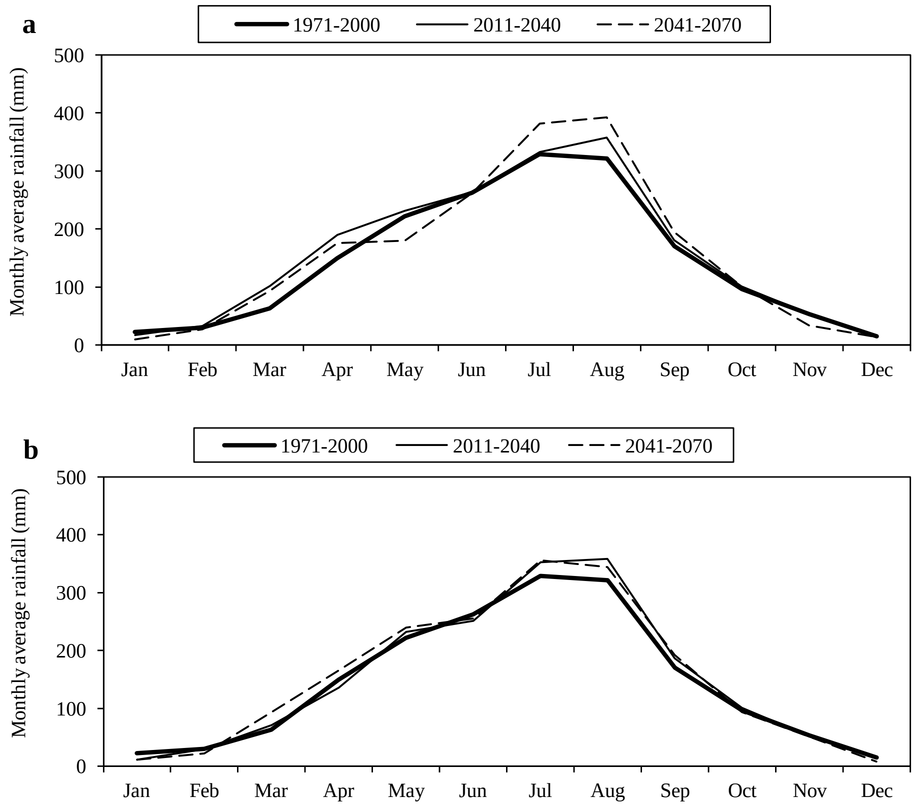

Fig. 2. Mean annual cycle of precipitation for present (1971–2000) and future (2011–2040 and 2041–2070) climate under **(a)** scenario A2 and **(b)** scenario B2.

HESSD
9, 3339–3384, 2012

Impact of climate change on sediment yield in the Mekong River Basin

B. Shrestha et al.

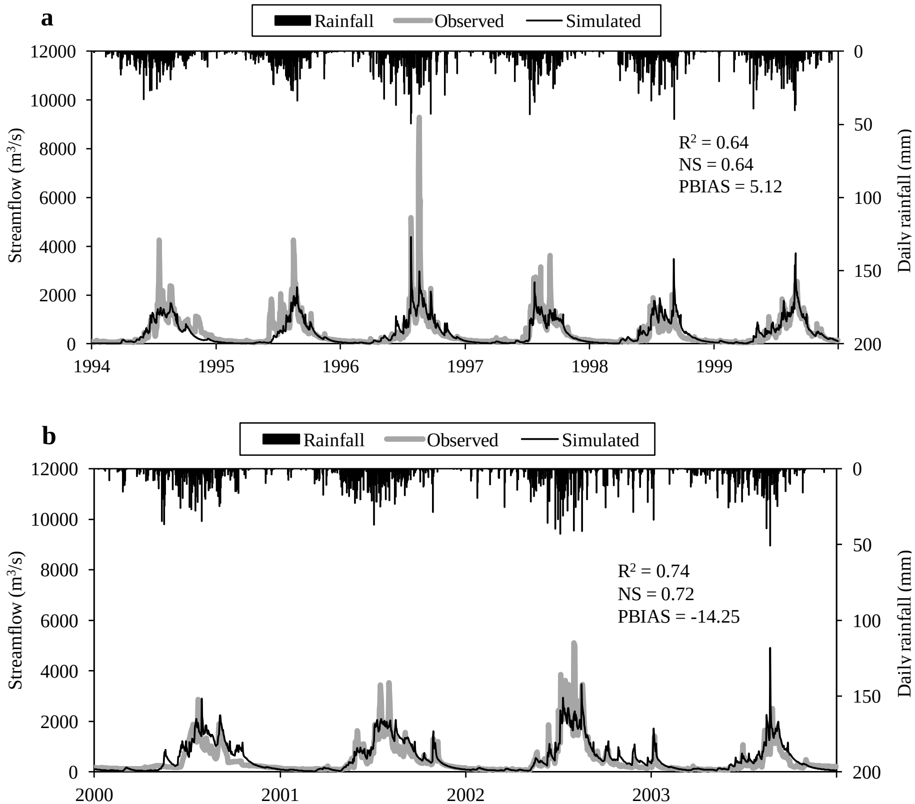

Fig. 3. Daily rainfall and comparison between measured and simulated daily flows for **(a)** calibration and **(b)** validation periods.

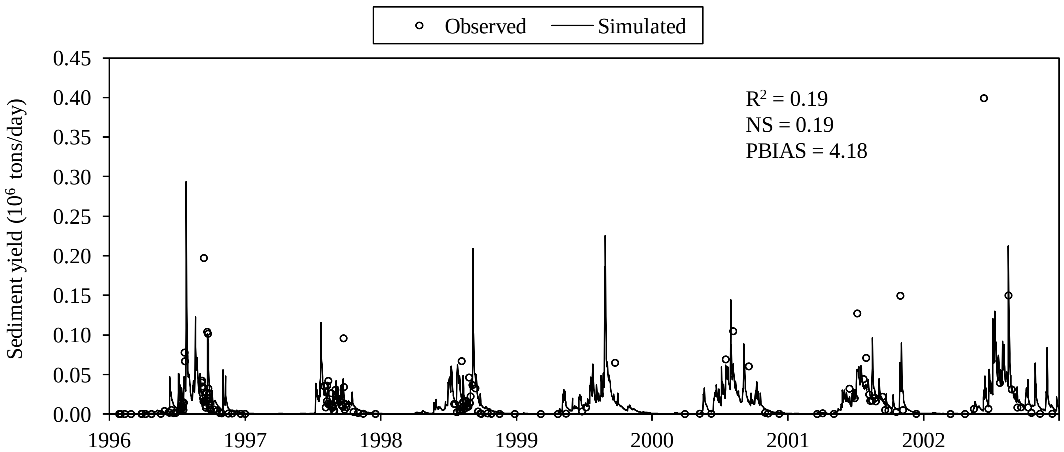

Fig. 4. Comparison between measured and simulated daily sediment yields for the calibration period.

HESSD
9, 3339–3384, 2012

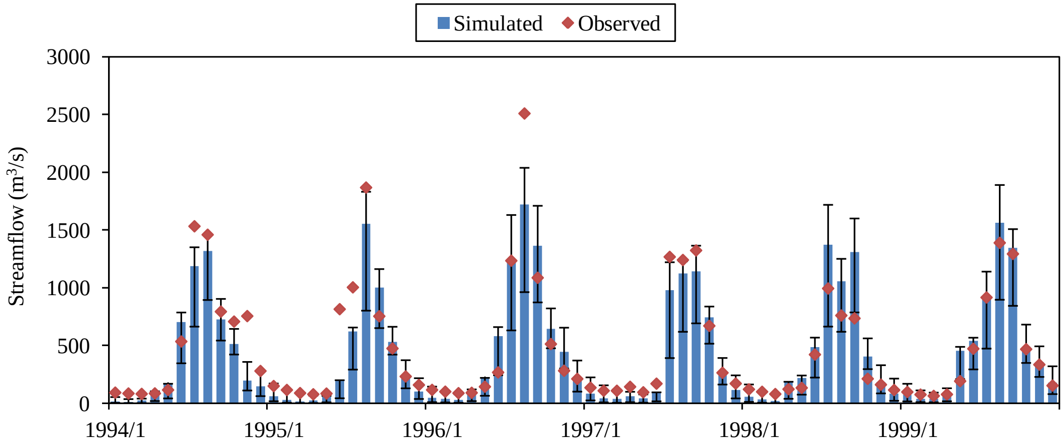

Fig. 5. Uncertainty analysis results of streamflow for the calibration period (The 95 PPU band is shown by thin black bars.).

HESSD
9, 3339–3384, 2012

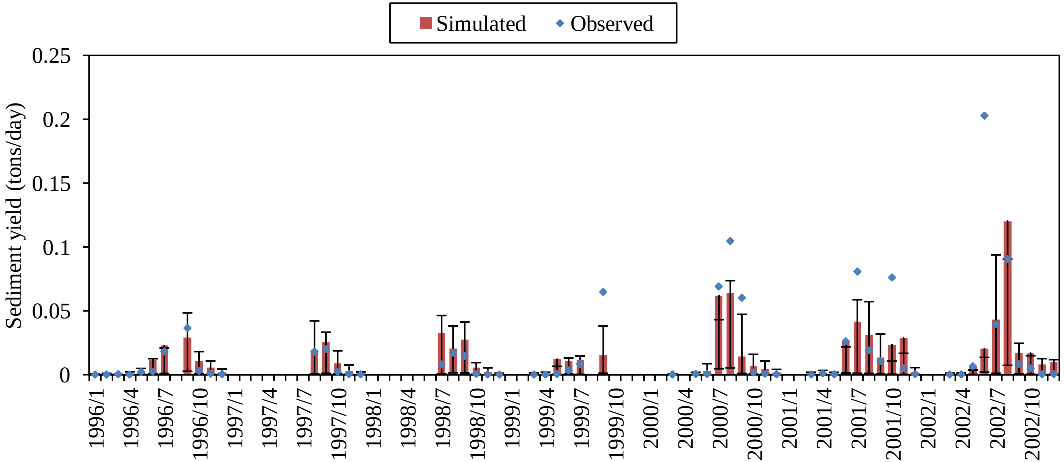

Fig. 6. Uncertainty analysis results of sediment yields for calibration period (The 95 PPU band is shown by thin black bars.) (Note: number of days used for calculating average sediment yield varies from 2 to 21.).

HESSD
9, 3339–3384, 2012

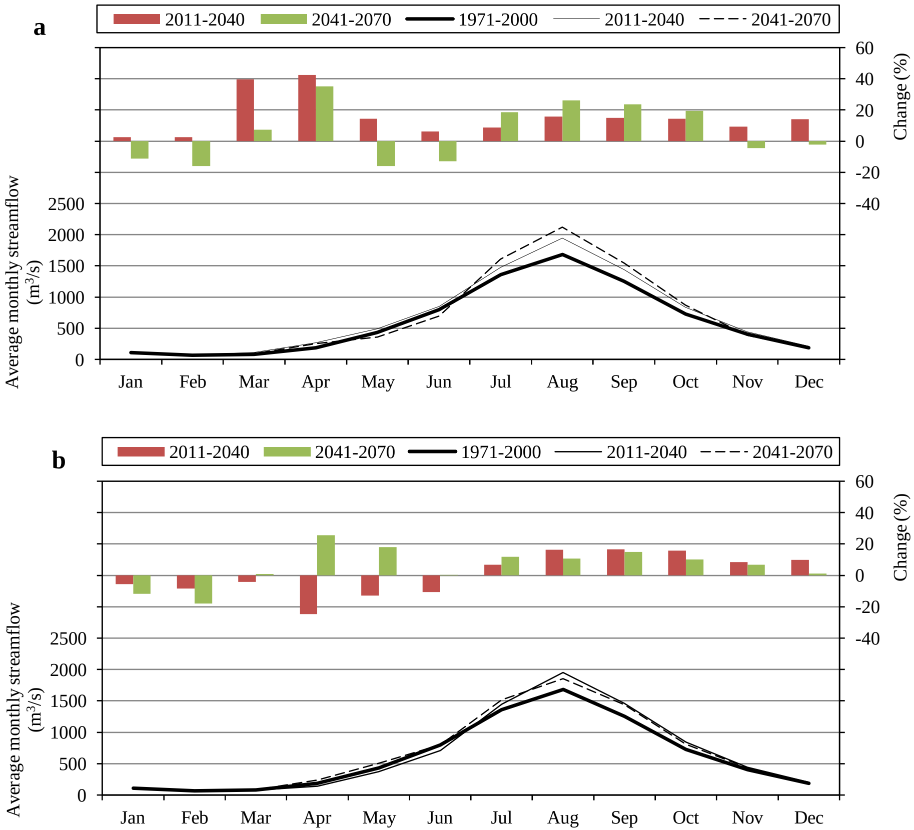

Fig. 7. Annual discharge cycle for present (1971–2000) and future (2011–2040 and 2041–2070) climates under **(a)** scenario A2 and **(b)** scenario B2; and change in future streamflow relative to 1971–2000 under **(a)** scenario A2 and **(b)** scenario B2. Note that lines represent average monthly streamflow and bars represent relative change (%) in streamflow.

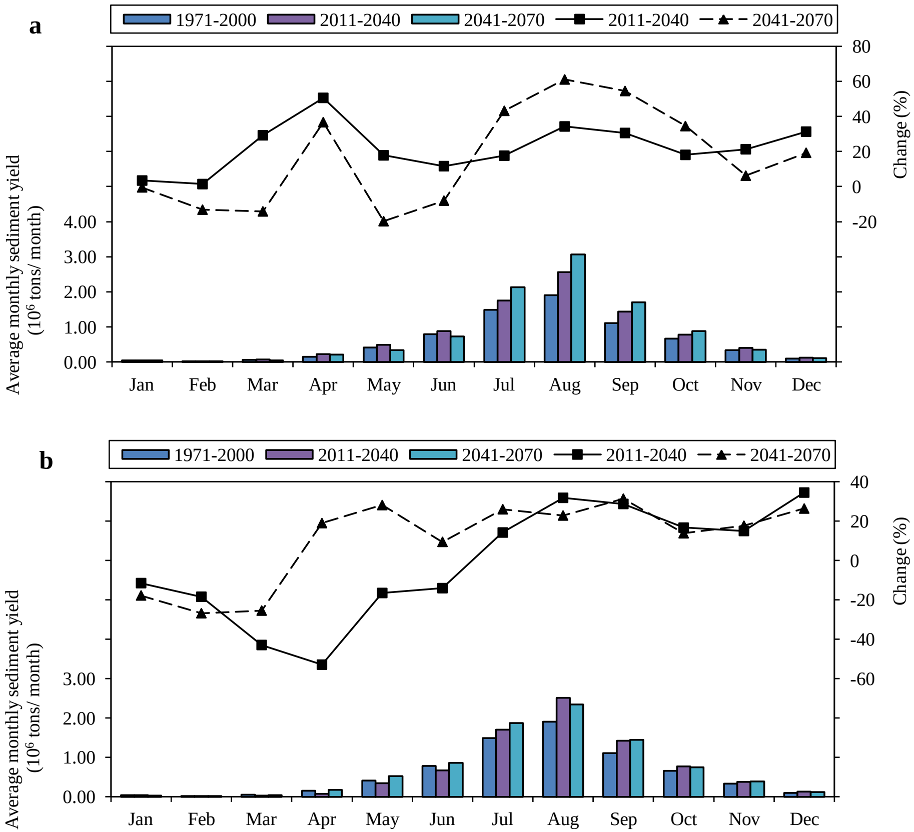

Fig. 8. Annual sediment yield cycle for present (1971–2000) and future (2011–2040 and 2041–2070) climates under **(a)** scenario A2 and **(b)** scenario B2; and change in future sediment yield relative to 1971–2000 under **(a)** scenario A2 and **(b)** scenario B2. Note that bars represent average monthly sediment yield and lines represent relative change (%) in sediment yield.

HESSD
9, 3339–3384, 2012

Impact of climate change on sediment yield in the Mekong River Basin

B. Shrestha et al.

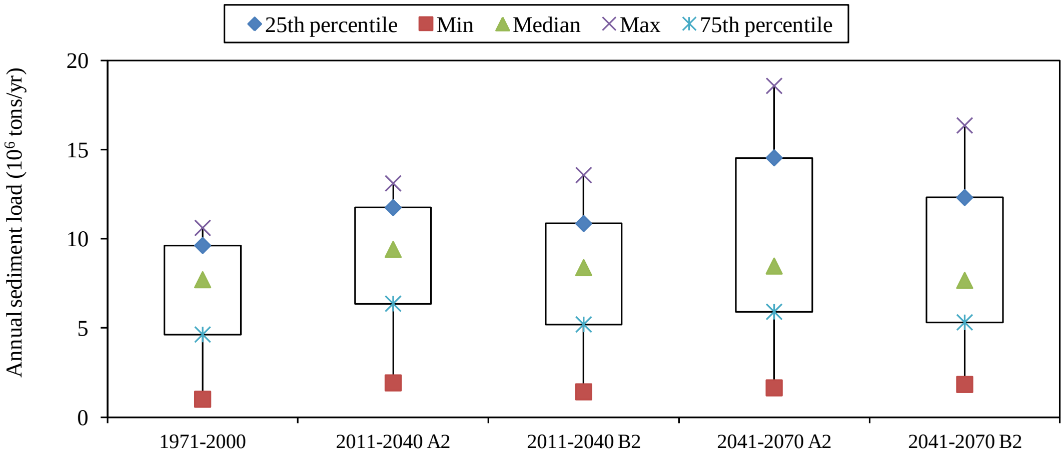

Fig. 9. Box-whisker plots of annual sediment load at gauging stations of Nam Ou for present climate (1971–2000) and future climate (2011–2040; 2041–2070) under scenarios A2 and B2.

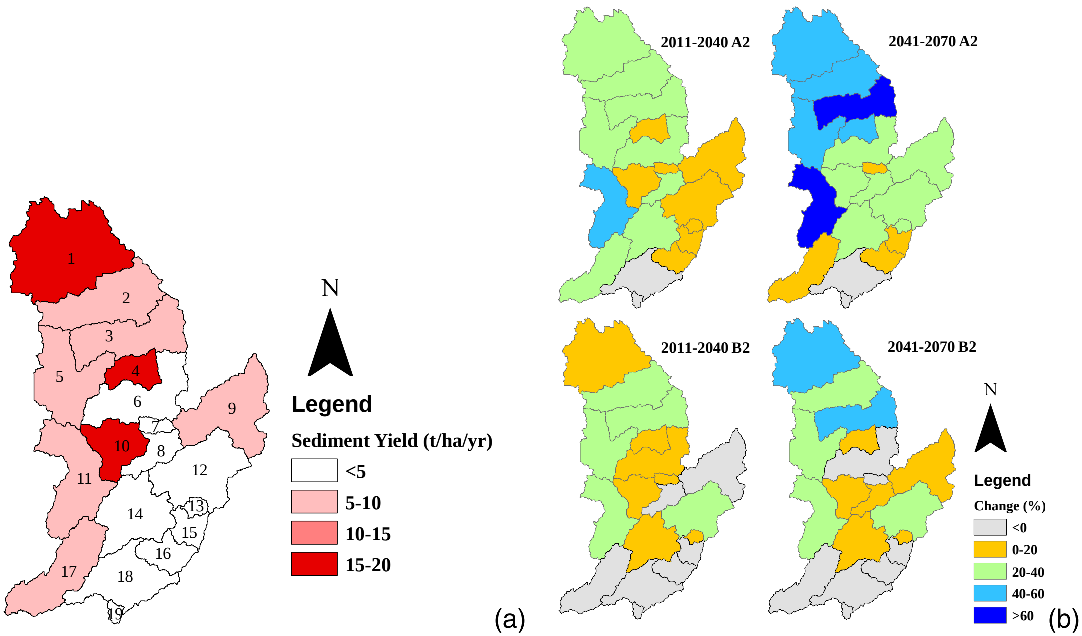

Fig. 10. **(a)** Average annual sediment yield from various sub-basins of the Nam Ou basin for present climate (1971–2000). **(b)** Relative changes in average annual sediment yield from various sub-basins under scenarios A2 and B2 as compared to 1971–2000.

HESSD
9, 3339–3384, 2012

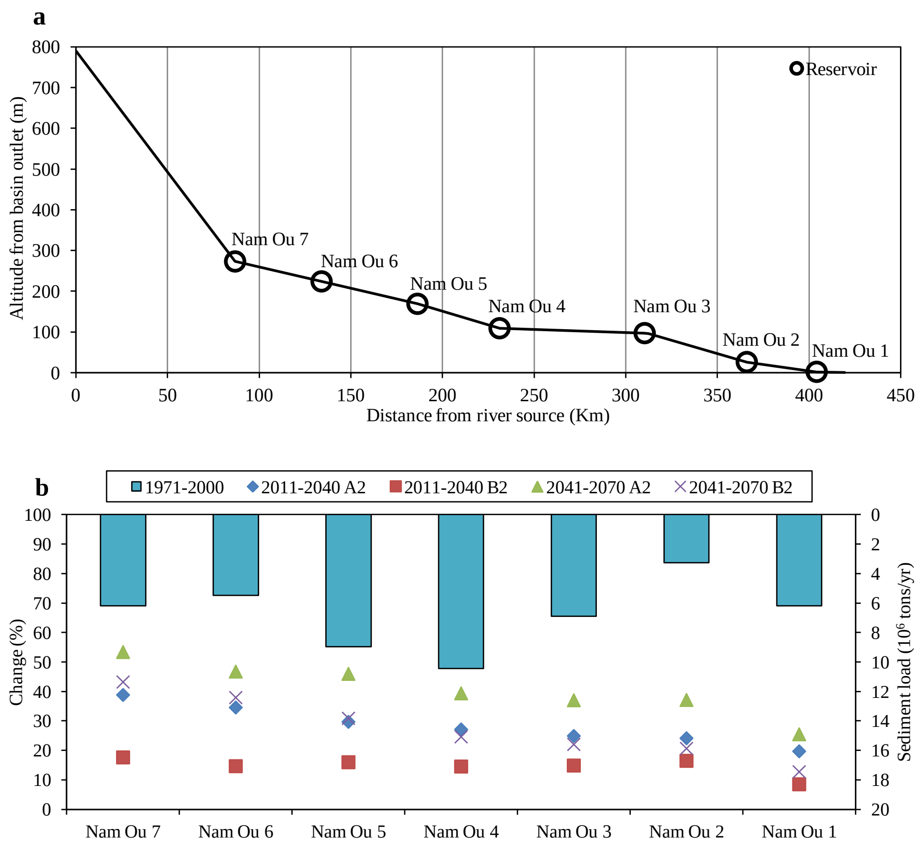

Fig. 11. (a) Longitudinal profile of the main stream showing the locations of planned reservoirs, and their elevation relative to the basin outlet datum. **(b)** Averages of simulated annual sediment load (1971–2000) at planned reservoir stations and relative changes in future sediment yield as compared to 1971–2000 under scenarios A2 and B2.

HESSD

9, 3339–3384, 2012